

Evaluating SMR Positioning with an Autostigmatic Microscope

Karlene Karrfalt^{a*}, Robert E. Parks^{b**}, Daewook Kim^{a,c}

^aWyant College of Optical Sciences, University of Arizona, Tucson AZ, USA

^bOptical Perspectives Group, LLC, Tucson AZ, USA

^cDepartment of Astronomy and Steward Observatory, University of Arizona, Tucson AZ, USA

ABSTRACT

An optical method of determining the location of the apex of a corner reflector mounted in a steel ball, commonly referred to as a Spherically Mounted Retroreflector (SMR), relative to the center of the ball to the 1-2 μm level was previously described by us. The method used an autostigmatic microscope focused on the apex and viewed the reflected spot image as the SMR was rotated about a normal to its entrance aperture. This measurement determined the lateral offset of the apex and tipping the SMR while viewing the spot gave an indication of the axial displacement.

A related questions arose recently, could the distance between two SMRs be determined to the same level of precision if the SMRs were rigidly mounted in a fixture so they could not be moved. We show the answer is yes assuming the stage moving the pair of SMRs has the required precision. As a SMR is scanned under the autostigmatic microscope the spot motion seen by the microscope is identical to that seen when scanning a spherical ball under the microscope and we have already shown that balls centers can be found to 1 μm precision using a 10x objective.

We show experimentally that we can determine the distance between 2 SMRs by repeated measurements to the 1 μm level by scanning over the SMRs rather than rotating. In fact, we can find the centers in x and y using just 2 data points within the aperture of the SMR.

Keywords: Spherically mounted retroreflector, SMR, Point Source Microscope, PSM, Autostigmatic Microscope

1. INTRODUCTION

The motivation for this paper was a question about calibrating a fixture, for what we think was a laser tracker, that used two spherically mounted retroreflectors (SMR)s spaced a precise distance apart¹. As the result of another inquiry², we knew we could locate the vertex of the cube corner reflector in a SMR with a Point Source Microscope (PSM)³, discussed in Section 2, by rotating the SMR in its kinematic locating nest⁴. In the case of the fixture calibration, the SMRs could not be rotated so the question became, could we find another method to measure the distance between apexes of the two SMRs.

Much before this time we had used the PSM to measure the distances between the centers of a row of precision balls pressed tightly against each other. By scanning the PSM across the row of balls while it was focused at the level of and in line with the centers of the balls, we could determine precisely when the PSM was centered over the balls in the scan direction. In this way we could determine the distance between the centers of the row of balls. Based on the paper written about finding the apexes of the cube corners in SMRs, we realized that scanning across a SMR would yield the same response from the PSM as if we were scanning solid balls. This paper is a documentation of that experiment.

We will first briefly describe the PSM used in both measurements and then show the previously unpublished results of scanning across the row of touching balls to demonstrate the method. Then we show the results of scanning across a ball and an SMR in the x and y directions to locate the ball and SMR centers. Finally, we show the results of scanning across a pair of SMRs to demonstrate the same kind of result as scanning across the solid balls. The main difference between the two cases was that the scan across the solid balls was a continuous motion with data being taken every 20-40 μm of scan while the measurement of the SMRs was done by manually moving the SMRs under a stationary PSM and taking data at a limited number of points.

Typical results of the two types of scans are shown to substantiate that the scans yield the same type of data. The data from the SMRs are better than the continuous scan of the solid balls because the data were taken carefully to prove a point while the solid ball scans were done to show feasibility of the method. We give an analysis of the SMR data to show the precision expected from similar SMR measurement as well as a couple of tips about how to make the measurements.

2. BACKGROUND

2.1 Autostigmatic microscope

The data taken for the solid ball and SMR scans were collected using a Point Source Microscope (PSM). A PSM is a classical autostigmatic microscope⁵ equipped with a single mode fiber pigtailed to a laser diode as the source and a digital camera to view the reflected images from the centers of curvatures and apexes of the optics being measured. Another key distinction of the classical autostigmatic microscope (ASM) is that internally it uses collimated light in the vicinity of the beam splitter. This means that when the microscope objective is removed, the PSM is an autocollimator as seen in Figure 1. Another way of thinking about the PSM is that it is an autocollimator with an objective so its focuses at a finite distance.

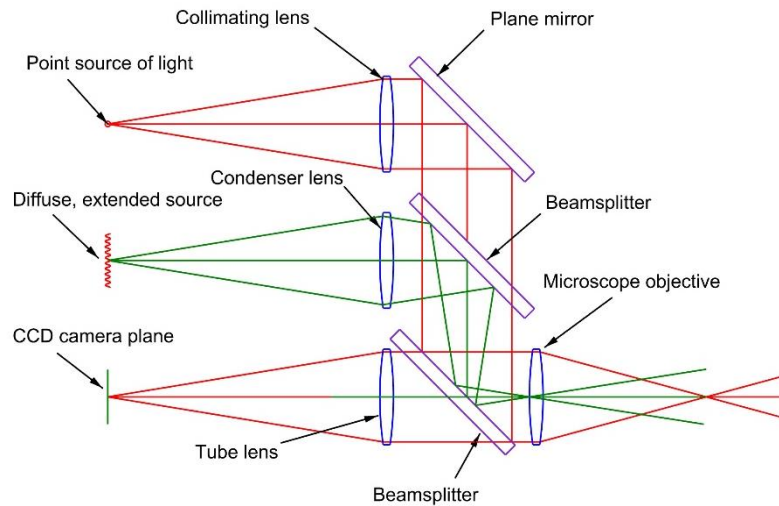


Figure 1. Optical ray paths in the PSM with the removeable microscope objective that converts it to an autocollimator.

The classical use of an ASM is the measurement of radii of lenses and mirrors. The ASM is first focused on the surface of the lens or mirror to get a Cat's eye image. This focus establishes where the mirror surface is axially and is used to establish the origin pixel laterally on the digital camera in the PSM because even if the surface is slightly tilted relative to the axis of the PSM, the reflected light spot always lands on the same origin pixel of the camera because that pixel is also conjugate with the fiber source and the image of the source on the mirror surface. Note also, when the fiber source is imaged on the surface, only one ray hits the surface at normal incidence. Rays in the light cone exiting the objective at the top of the aperture are reflected through the bottom because the angle of incidence equals angle of reflection.

After focusing the PSM on the surface of the optic, the PSM is then moved away from the mirror, in the case of a concave mirror, to a point where the focus of the objective is near the center of curvature. The PSM is moved in x, y and z until there is a well focused return spot on the origin pixel of the camera. In this condition, every ray in the cone of light incident on the mirror from the objective focus at the center of curvature is normal to the surface of the mirror.

As the PSM is moved one unit in x or y from the center of curvature the reflected spot moves 2 units on the PSM camera as seen in Figure 2. This means that as the PSM scans across the ball the reflected spot appears to move twice as fast as the scan speed. Figure 2 also shows the case for scanning the PSM past a hollow 90° prism, an analog for a cube corner that is easier to draw in 2 dimensions and behaves from the PSM vantage point the same as a hollow cube corner. Again, the reflected spot moves twice as fast as the scan. Figure 2 is exaggerated for clarity of the ray paths in the ball and cube

corner. For the rays reflected into the objective, think about the shift in terms of object height. Then it is clear the effect is the same on image height at the camera for both ball and cube corner.

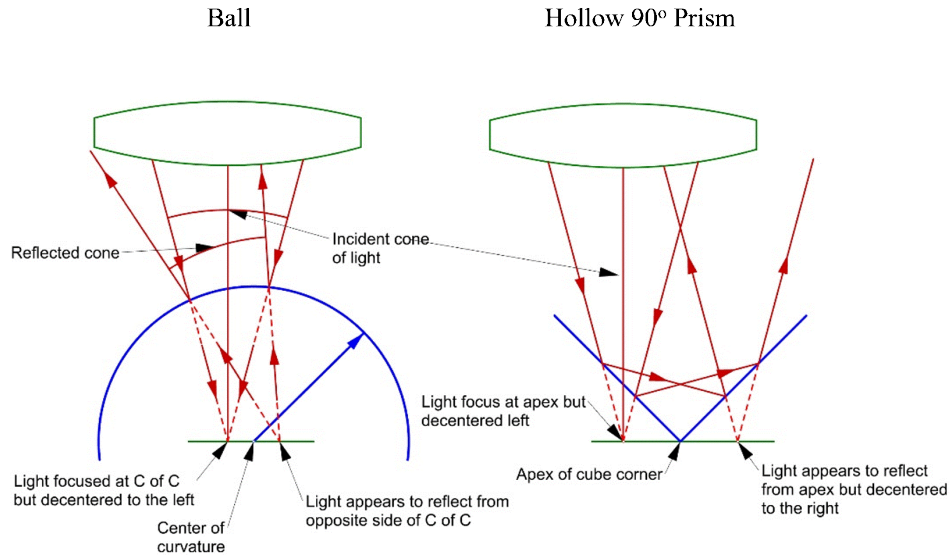


Figure 2. The effect of decentered cones of light incident on a ball or hollow 90° prism on the reflected cones.

2.2 Opto-mechanical alignment and measurement with an autostigmatic microscope

Some years ago, one of us (RP) did an experiment where a PSM was continuously scanned over a row of 1" diameter, Grade 5 balls. The balls were constrained to lie in a straight line and positioned so that they touched each other. The experimental set up is shown in Figure 3(a). The vertical row of balls is on the left of the setup. A right angle fold mirror was used on the PSM so the objective was facing the balls while the PSM moved vertically.

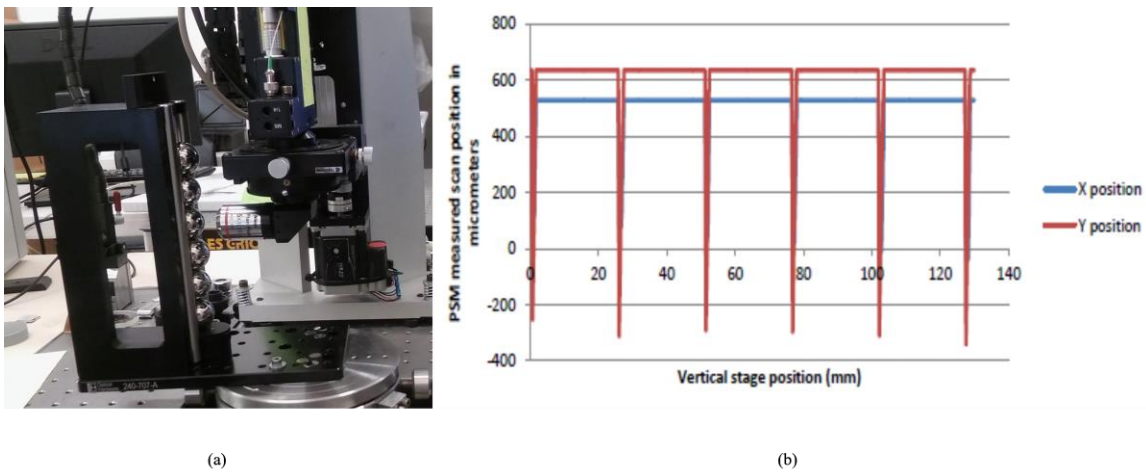


Figure 3. (a) (left) Ball scanning experimental setup. (b) (right) Data from the scan over the row of balls.

This experiment was done simply to show the feasibility of doing a continuous scan over a row of balls but is useful for introducing the similar concept of scanning over a set of SMRs. Figure 3(b) shows the PSM data output where ball center of curvature locations was sampled in intervals between 20 and 40 μm apart over the slightly more than 125 mm distance between the outer most ball centers. The red curve shows the ball center locations in the scan direction. Obviously, no light got to the camera except very near the ball center so the data around 630 μm is dead time in the scan. The ball centers are the spikes in the -300 μm region. The blue curve is the ball center in the cross scan direction. The visible part of this data at about 540 μm is dead time and the actual ball center data is hidden behind the orange curve.

Figure 4 shows a 2 mm portion of the scan over the 2nd ball in the row. At about 25.8 mm along the scan light starts getting into the objective so the PSM centroiding algorithm tries to find a centroid. It is not until 26.1 mm or so, however, that a good image is found which tracks across the camera in a way expected from the rays in Figure 2. At approximately 26.7 mm the light is moving out of the microscope objective and the centroiding moves to dead time. In the interval between 26.1 and 26.7 mm the centroid crosses the origin (0 mm) of the the PSM camera in the scan direction (orange curve). The cross scan position of the centroid (blue curve) remains nearly constant at about 80 μm .

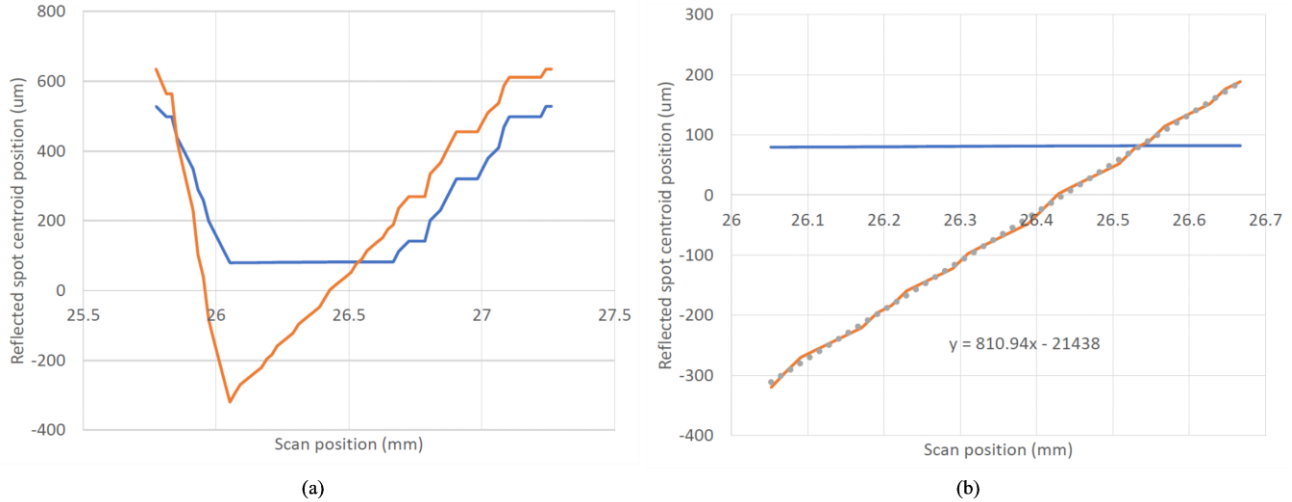


Figure 4. (a) (left) Reflected spot centroids in scan (orange) and cross scan (blue) positions versus scan position. (b) (right) Linear fit of spot centroid in scan (orange) and center portion of cross scan (blue) positions versus scan position (blue).

If we look just at the portion of the scan in the vicinity of the origin, we see there is no data precisely at the origin but that the centroid moves linearly. This enables one to extrapolate the zero crossing as 26.436 mm. We can then use the scan direction zero crossing to solve for the cross scan centroid position at that same instant from a linear fit to the cross scan data to get a ball center of 81 μm .

The result of scanning all 6 balls where the zero crossing was calculated as described above is shown in Figure 5(a). The rather uninteresting Figure 5(a) shows a scaling error that translates to about a 75 μm error over the 125 mm scan that is probably in the leadscrew of the stage.

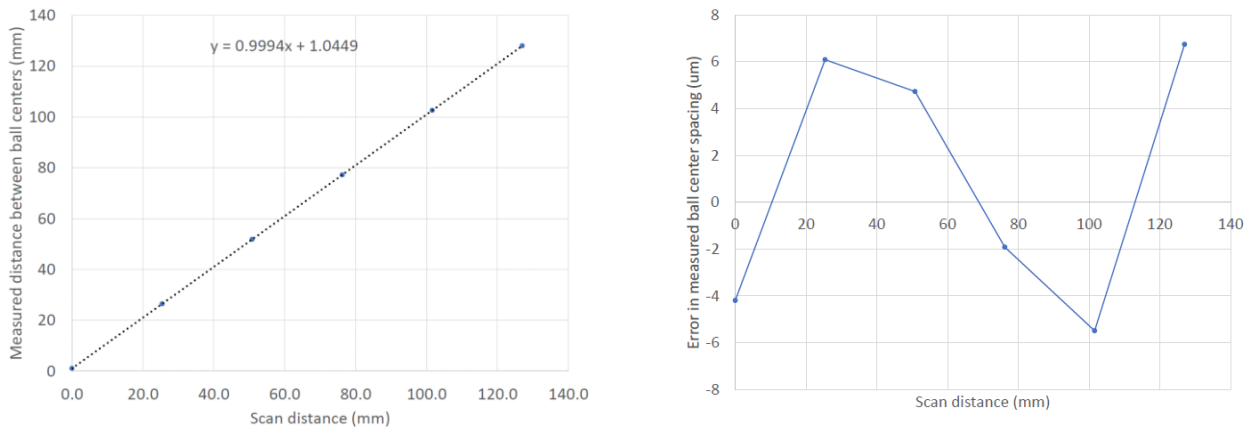


Figure 5. (a) (left) Measured distance between ball centers versus scan distance. (b) (right) residual error in measured ball spacing after removing the best linear fit.

There was little error in the balls themselves as they were Grade 5, that is, within their nominal 25.4 mm diameter to 125 nm. Figure 5(b) shows the residual error in ball centers after removing the linear fit in Figure 5(a). This error is about ± 6

μm with the balls on the ends of the row the worst offenders. As stated above the data were taken at intervals of 20 to 40 μm and the entire 125 mm scan took 2 minutes at a constant velocity.

The real significance of this data is that, no surprise, the reflected spot moves linearly with the scan motion in the regions where the reflected light gets back into the PSM objective. With a little thought about this consequence, it means that only two data points are needed per ball to fully locate the ball center in both the scan and cross scan directions. This has particular significance when it comes to scanning SMRs.

3. EXPERIMENTAL SET UP

The remainder of the paper now shifts to our experiment which shows that one can find the SMR center by employing a similar scanning technique as that described in Section 2. Our experiment was conducted in two parts. First it is shown that scanning with a PSM over a ball produces the same result as scanning with a PSM over a SMR in both the x and y directions, that is, the reflected spot moves linearly with the scan motion. The x and y scan planes are shown in Figure 6(c). First part of experiment used one 3 ball kinematic mount on two cross mounted digital micrometer stages.

Before scanning over the ball and SMR, the PSM and translation stages were aligned to each other in both the scan and cross scan directions by centering the confocal reflected spot from the ball's center to the center of the PSM crosshairs. Once the ball was aligned to the PSM, the digital micrometer translations stages were zeroed.

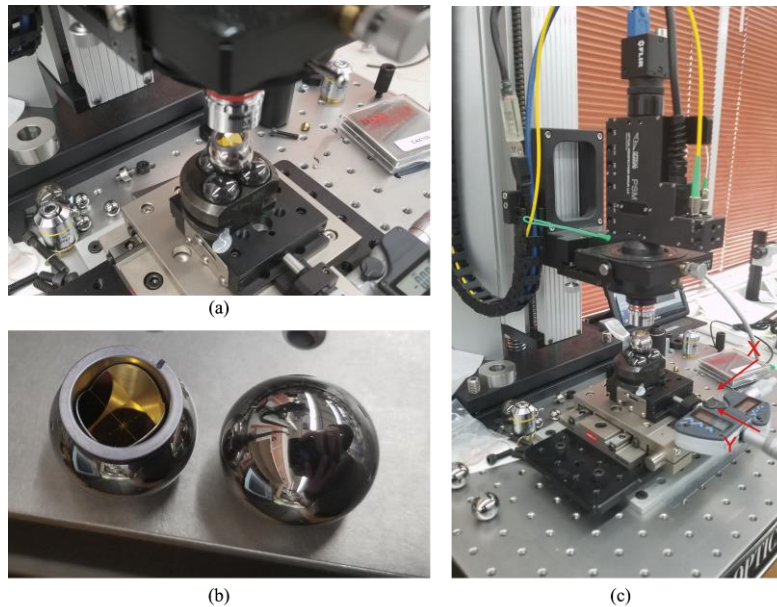


Figure 6. (a) SMR in kinematic mount, (b) close-up image of SMR (left) and sphere(right), (c) PSM set up for SMR scan measurements. The x and y scan planes are shown in red.

Next, with the micrometer translation stages aligned to the PSM, the ball was manually translated across the PSM in the x direction and the reflected centroid position was recorded by the PSM. Approximately 10 measurements were taken, and the corresponding micrometer positions recorded. This scanning procedure was then repeated in the y direction. Then the ball was replaced by an SMR and the procedure was repeated. As seen below in Figs. 8 and 9 scanning either ball or SMR give essentially the same results, a linear motion of the reflected spot relative to the micrometer stage in both directions with a slope of roughly 2 indicating the reflected spot moves twice as fast as the ball or SMR. In fact, scanning either artifact is an ideal method of calibrating the spatial scale of the PSM. More importantly, the motion is completely linear in both cases so that it is not necessary to take more than 2 data points to determine where the ball center or SMR apex is relative to the micrometer stage.

For the second part of our experiment, two kinematic mounts (SMR nests) were attached to an aluminum plate at approximately 24.6 mm apart. This set up is shown in Figure 7. The right hand position (ball 1) was aligned to the center of the PSM as in the first part of our experiment. The relative position between the right hand (ball 1) and left hand (ball 2) positions were then measured by positioning the focus spot of the objective at the center of the ball as was described in

Section 2.1. Finally, the balls were replaced by two SMRs and the scanning procedure described earlier in this section was used to determine the x position of each SMR relative to the other.

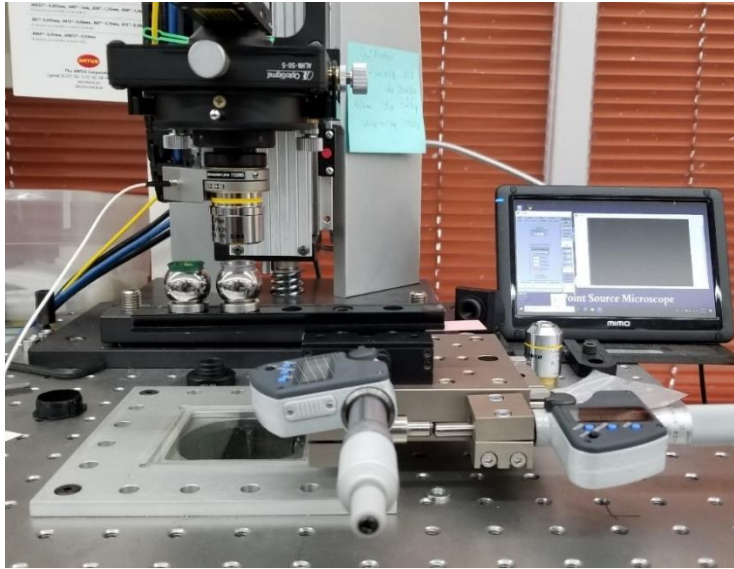


Figure 7 Set up for SMR relative position measurements. PSM was used to measure the reflected spot centroid from the scans of SMR 1(left SMR) and SMR 2 (right SMR)

4. EXPERIMENTAL DATA AND ANALYSIS

4.1.1 Measurement to show that ball and SMR behave similarly when scanned with the PSM

As was described in Section 2.2, the ball position of the PSM measurements were plotted against the micrometer scan position measurements to extrapolate the position of the ball and SMR. A linear fit was then applied to the data. The fit for the data is shown in Figure 8. In an ideal case one would expect the slope of the linear fit to be 2 as the reflected spot travels at twice the rate of the ball due to the reflected ray being at an angle twice that of the incident angle. From the linear fit of the data one can see that the slopes are approximately -1.99. The deviation of the slope value from the ideal is attributed to the calibration factor of the PSM being slightly off. The negative sign results from the positive direction of the micrometer scan being opposite to the scan direction of the PSM.

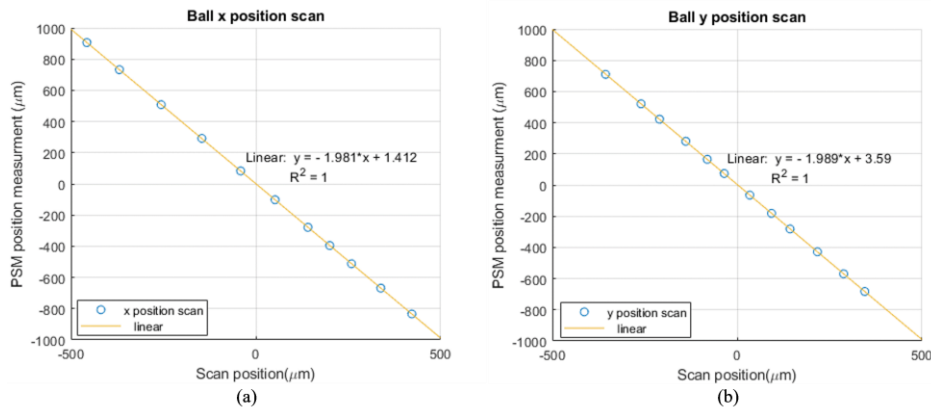


Figure 8. (a) (left) Ball x position scan and linear fit. (b) (right) Ball y position scan and linear fit.

The position of the ball center is then determined by solving the linear fit equation for the zero intercept of scan position axis. Using this method, the ball center is measured to be at $x = -0.7 \mu\text{m}$ and $y = -1.8 \mu\text{m}$. The R^2 value of 1 is expected for the ball.

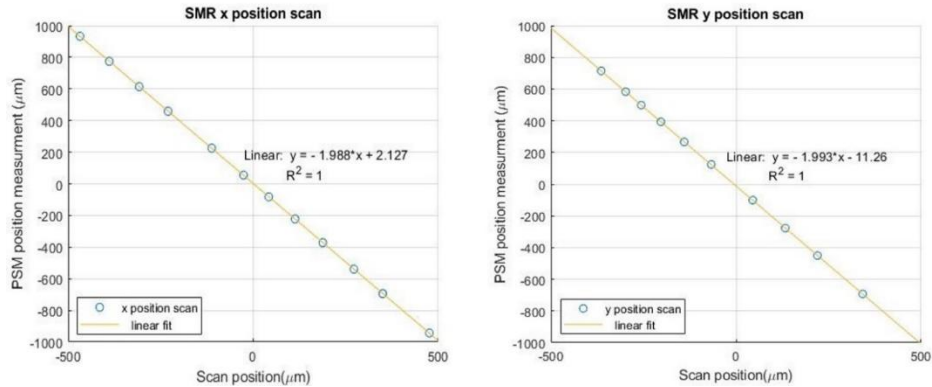


Figure 9. (a) (left) SMR x position scan and linear fit. (b) (right) SMR y position scan and linear fit

Next this procedure was applied to the SMR scan data as shown in Figure 9. The SMR center is measured to be at $x = -1.1 \mu\text{m}$ and $y = +5.7 \mu\text{m}$. Again, the R^2 value of 1 indicates a good linear fit for the SMR scan, the desired result. Since both the ball and SMR were measured in the same SMR kinematic nest, the measured apex of the corner reflector was decentered by about $7 \mu\text{m}$ but the azimuthal orientation was not noted. The position of the ball and the SMR centers are shown in Table 1.

Table 1. Calculated position of the sphere’s center and SMR’s center

Center position	x (μm)	y (μm)
SMR	-1.1	+5.6
Ball	-0.7	-1.8

The linear fit is particularly important for the SMR because a measurement cannot be made at the precise location of the apex because of inevitable manufacturing flaws at the apex as seen in Fig. 10. Further, measurements are corrupted of the reflected beam lands on contamination, and its mirror image, that tends to be worse in the vicinity of the apex. Also, the joints between mirror surfaces interfere with making good measurements.

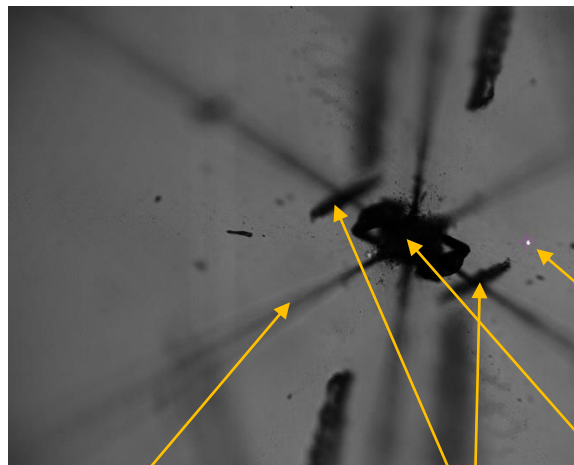


Figure 10. Image of a SMR in the vicinity of the apex showing the manufacturing flaws at the apex. The bright spot is the reflected imaged. Also shown are the joints between mirror sections and mirrored contamination.

4.1.2 Measurements to show that the ball center is correctly calculated from two data points

Even though we justified finding the center of the ball via linear interpolation in Section 2.2, we had the opportunity to show this explicitly in the next experiment. Two SMR nests were attached to a bar approximately 25 mm apart and the bar was mounted on a 1" travel stage and adjusted so that the centers of the nests could both be reached within the 1" travel. Two 7/8" steel balls were set in the nests so their centers and separation could be measured. The ball diameters were chosen because the SMRs were the same diameter and SMRs could be swapped for balls without having to make any other adjustments to the setup.

Sets of 3 measurements were made on each ball, one at the center of the ball within 1 μm and 1 each on either side of center at arbitrary distances about 200 μm on either side of center. The 2 measurements on either side of center were used to calculate where the center of the ball was in the scan and cross scan directions. The ball was not translated in the cross scan direction, but the ball centers were not perfectly aligned in cross scan but close enough that the lack of alignment (about 80 μm) would not affect the distance in the scan direction. The results are shown in Table 2 where the units are mm.

Ball 1					Ball 2				
x micrometer	x calc cen	x PSM spot	y PSM spot	y calc cen	x micrometer	x calc cen	x PSM spot	y PSM spot	y calc cen
0.288		-0.574	-0.064		24.891		-0.425	0.012	
0.001	0.0010	0.000	-0.086	-0.0863	24.678	24.6785	-0.001	-0.004	-0.0042
-0.177		0.356	-0.100		24.491		0.375	-0.018	
0.250		-0.497	-0.068		24.9		-0.441	0.012	
0.001	0.0012	0.001	-0.086	-0.0869	24.679	24.6790	-0.001	-0.005	-0.0042
-0.197		0.396	-0.102		24.493		0.371	-0.018	
0.251		-0.499	-0.068		24.894		-0.430	0.010	
0.001	0.0012	0.000	-0.087	-0.0873	24.678	24.6787	0.000	-0.006	-0.0059
-0.163		0.328	-0.100		24.501		0.355	-0.019	

Table 2 Centers in x and y of 2 solid steel balls spaced about 24.677 mm apart as determined by 2 reflections from each ball showing that the calculated center matched the value measured at the ball center. All units are mm.

In Table 2 the x micrometer data are the readings off the digital micrometer moving the ball in the scan direction. In none of the measurements was the ball or SMR moved cross scan in y. X calc cen is the calculated x ball center using the two x micrometer and x PSM spot readings either side of center. The ball center measurement is the highlighted row showing the measured center as well as the calculated center. The x and y spot data are from the PSM and the y calc cen is the calculate ball center y value at the calculated x center. Y calc cen uses the x micrometer and y spot readings along with the calculated x center value. The measurements were done 3 times moving from Ball 1 position to Ball 2. The values are organized in the Table, so the values are easier to compare, but the data were taken Ball 1 to Ball 2 and then back to Ball 1 for the next set.

In every case the calculated ball center in x and y is within 1 μm of the measured value showing that the method of calculating both centers is valid and precise. In addition, we can take the ball centers as the centers of the nests so that when SMRs are substitute for the balls there is a reference for where the apexes should be located assuming perfectly centered SMRs.

4.1.3 Measurements showing SMR centers

SMRs replaced the balls in the 2 nests and the measurements were repeated as with the balls except that no measurement was taken at the SMR center because of the flawed apex, just a measurement either side of the center. The data is shown in Table 3 displayed in the same way as Table 2 for easy comparison except there is no data for the measured SMR center, only a calculated value. Again, in both x and y the data for the 3 measurements are the same within 1 μm .

SMR 1					SMR 2				
x micrometer	x calc cen	x PSM spot	y PSM spot	y calc cen	x micrometer	x calc cen	x PSM spot	y PSM spot	y calc cen
0.214		-0.430	-0.066		24.904		-0.453	0.004	
	0.0004			-0.0841		24.6783			-0.0124
-0.163		0.329	-0.098		24.463		0.432	-0.029	
0.240		-0.479	-0.065		24.903		-0.450	0.005	
	0.0013			-0.0838		24.6780			-0.0126
-0.216		0.436	-0.101		24.490		0.376	-0.027	
0.182		-0.362	-0.070		24.925		-0.495	0.006	
	0.0012			-0.0844		24.6784			-0.0131
-0.206		0.415	-0.101		24.498		0.362	-0.027	

Table 3 A measurement like that in Table 2 but on SMRs of the same diameter and measured at 2 points. Units are mm.

4.1.3 Comparison of ball and SMR centers

Table 3 shows the x and y centers of the two ball and two SMRs. The difference between Ball 1 and SMR 1 are relatively small but the difference between Ball 2 and SMR 2 are larger and mostly in the y direction. Looking at the Ball 1 and 2 differences we see the x distance between ball and SMR are virtually the same, but there are significant differences in the y direction. The difference in y between the two balls is attributed to the bar on which the nests were fastened not being perfectly aligned to the x direction of the stage motion so Ball 2 is 82 μm closer to the origin of coordinates in the 24.677 mm of stage motion. SMR 2 also moves in the same direction but not as much by about 11 μm . All of this implies that the apexes of the two SMRs were quite well centered in the x direction, quite by chance, but the apexes of both SMRs were decentered in the y direction. We know that these differences are not measurement error because the rss'd standard deviations of the differences are all $< 1 \mu\text{m}$.

	x	y		x	y	x diff	y diff
Ball 1	0.0011	-0.0868	Ball 2	24.6787	-0.0048	24.6776	0.0821
SMR 1	0.0010	-0.0841	SMR 2	24.6782	-0.0127	24.6772	0.0714
diff	0.0002	-0.0027		0.0005	0.0079		

Table 4 Differences in the centers of balls and SMRs constrained in the same kinematic nests. Units are mm.

4.1.3 Test of hypothesis that the apex of SMR 2 is decentered in the y direction

To see if there was a decenter of the apex of SMR 2 the SMR was rotated approximately 180 degrees and the test repeated. Table 5 shows the values of the center of SMR 2 in its initial position for all previous data and rotated about its azimuth approximately 180 degrees.

	x center	y center
SMR 2	24.6782	-0.0127
SMR 2 rot	24.6773	0.0022
diff	0.0009	-0.0149
std dev	0.0003	0.0005

Table 5 Center coordinates of SMR 2 as initially positioned and rotated about 180 degrees

From Table 5 we see the apex of SMR 2 is decentered in the y direction because of the large difference in the y center with rotation. There is also a small decenter in x. The x and y decenters will add vectorially but since the y decenter is much larger than the x we can ignore x and just concentrate on the y decenter. The difference of about 15 μm is the

result of a rotation so this is double the motion recorded by the PSM which is already twice the apex decenter. This means the apex decenter is $< 4 \mu\text{m}$. Because we did not also rotate and measure SMR 1 we cannot completely explain the results of the difference in Table 4 but the y decenter in SMR 2 was large contributor to the difference. It is also clear that this method of locating the apexes of SMRs is quite sensitive to the decenters of the apex.

5. APPLICATION OF THE SCANNING METHOD

While this application does not apply to SMRs, it is closely related to scanning balls and calibration in general. Several years ago, we showed you could make a virtual ball plate⁶ by printing an array of concentric Fresnel zones on a photomask substrate as in Fig. 11 a. When a particular radius Fresnel zone was interrogated by a PSM focused at the Fresnel zone virtual radius of curvature the Fresnel zone created a focused spot on the PSM detector exactly as if it were focused on the center of a ball. Because each of the concentric Fresnel zones had a different radius of curvature there were 4 planes of centers of curvature parallel to the virtual ball plate photomask as illustrated in Fig. 11 b. In this case, a PSM was attached to the spindle of a CNC mill and programmed to pause at the center of curvature of each zone once the photomask and machine coordinate systems were aligned to each other. The PSM recorded the x, y location of the center of curvature at each location the CNC paused. This gave data to plot the error between the CNC location and the PSM measured location of what should have been the same position in space. Fig 11 c shows this error map where the light gray regular pattern is the perfect set of locations and the distorted grid the mapped locations at 3 planes above the photomask where the scale of the errors was magnified by a factor of 1000.

Bases on the work already described, we believe the photomask virtual ball plate could be interrogated in a continuous scan pattern rather rapidly.

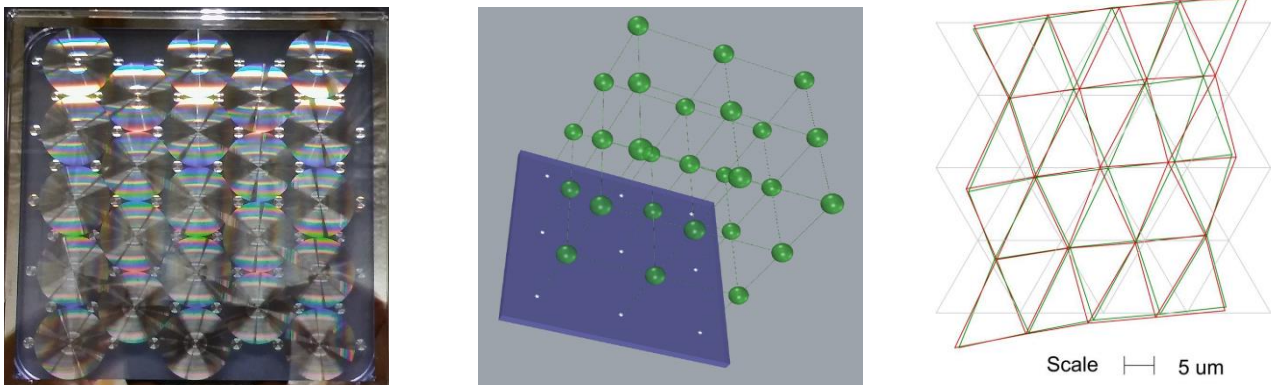


Fig. 11a (left) Virtual ball plate photomask array of 23 patterns of 4 concentric Fresnel zones of 4 different radii of curvature, Fig. 11b (center) Diagram of virtual centers of curvature in planes above the photomask. Fig. 11c Error map of the distances between the locations of the photomask centers of curvature and the CNC machine programmed locations.

6. CONCLUSIONS

We began by reviewing some older, unpublished work showing that a row of solid balls could be continuously scanned by optical means to find their centers with $1 \mu\text{m}$ level precision. We also reviewed previous work where we found the apexes of SMRs to the same sort of precision by rotating the SMR and measuring the shift in reflection from a light beam focused in the plane of the apex. This led us to see if the apexes of SMRs could be found by scanning instead of rotating and a simple drawing of how rays propagate through a SMR lead us to the conclusion that scanning would work if we could show that as in the case of solid balls the reflected beam moved linearly with translation of the SMR through the beam. This was clearly demonstrated to be the case by experiment.

Because the reflection is linear with motion, only two data points are needed to locate the apex of the cube corner in a SMR, a decided advantage in the case of SMRs as the location of their apexes are not directly measurable due to manufacturing flaws. We found that the apex of an SMR can be found in the plane of the aperture of the SMR to at least

1 μm precision in both x and y using just 2 data points in the aperture. This leads to the possibility of finding the centers of the apexes of SMRs by scanning along a row of SMRs with continuous motion.

REFERENCES

- [1] Private communication with Christian Guertin, Vermont Photonics
- [2] Parks, R. E., "What is a PSM?", https://optiper.com/multimedia/what_is_a_psm.mp4
- [3] Private communication with Joe Gleason, Baltec Div. of Micro Surface Engr., Inc.
- [4] Parks, R. E., "Prism alignment using the Point Source Microscope", Proc. SPIE, **11103**, 1110303 (2019)
- [5] Steel, W. H., "The Autostigmatic Microscope", Optics and Lasers in Engineering, **4**, 217-27 (1983)
- [6] Parks, R. E., Ziegert, J. and Groover, J., "Computer Generated Holograms as 3-Dimensional Calibration Artifacts", Proc. ASPE Annual Meeting, 117-20 (2017).